Three-dimensional Hybrid-PIC Simulation of Microwave Neutralizer

IEPC-2013-098

Presented at the 33rd International Electric Propulsion Conference,
The George Washington University • Washington, D.C. • USA
October 6 – 10, 2013

K. Kubota[1]
Japan Aerospace Exploration Agency, Chofu, Tokyo, 182-8522, Japan

H. Watanabe[2], I. Funaki[3]
Japan Aerospace Exploration Agency, Sagamihara, Kanagawa, 252-5210, Japan

N. Yamamoto[4], H. Nakashima[5]
Kyushu University, Kasuga, Fukuoka, 816-8580, Japan
and

T. Miyasaka[6]
Gifu University, Gifu, Gifu, 501-1193, Japan

Abstract: In order to analyze a microwave neutralizer in ion's time/space scales, weakly coupled simulations of a Hybrid-PIC (Particle-In-Cell) and an electromagnetic PIC simulation were conducted. The ionization rate with respect to microwave discharge was obtained from the electromagnetic PIC solver, and was exported to the Hybrid-PIC where ions and electrons were dealt with particles and fluid, respectively. Two anode potentials of 20 and 38 V were examined to simulate a transition from a low current mode to a high current mode. The electron temperature inside an orifice was fixed to 3 eV at the low current mode, and was artificially increased to 4 eV at the higher anode potential of 38 V. It was found that the grown ion density inside the orifice at the high current mode leads to increase in the ion density around the antenna, and hence to increase in ion production rate by microwave discharge. As a result, the electron current collected by the virtual anode was increased from 22 mA to 98 mA.

Nomenclature

B	=	magnetic flux density
C	=	thermal velocity
E	=	electric field
e	=	elementary charge
H	=	magnetic field
j	=	current density
m	=	mass of particle

[1] Researcher, Institute of Aeronautical Technology, kubota.kenichi@jaxa.jp
[2] Research Fellow, JAXA's Engineering Digital Innovation Center, watanabe.hiroki@jaxa.jp
[3] Associate Professor, Institute of Space and Astronautical Science, funaki@isas.jaxa.jp
[4] Associate Professor, Department of Advanced Energy Engineering Science, yamamoto@aees.kyushu-u.ac.jp
[5] Professor, Department of Advanced Energy Engineering Science, nakasima@aees.kyushu-u.ac.jp
[6] Associate Professor, Department of Human and Information Systems, miyasaka@gifu-u.ac.jp

n = number density
P = input power
p = pressure
R = gas constant
T = temperature
t = time
u = velocity of fluid
v = velocity of a particle
x = coordinate

β = Hall parameter
φ = electric potential
μ = mobility
ν = collision frequency

subscripts

a : anode
e : electron
h : heavy particle (neutral and ion)
i : ion

I. Introduction

The ion engine μ10 installed on the Japan's asteroid explorer HAYABUSA established the availability of microwave discharge for electrostatic propulsion system. On that explorer, four ion engines were equipped, and each engine generated a thrust of 8 mN, a specific impulse of 3,200 seconds, and consumes an electric power of 350 W. In 2005, the HAYABUSA landed on asteroid ITOKAWA, and accomplished the first ever round trip space flight between Earth and an asteroid.[1] In the actual operation, however, the life time of one of the ion engines was restricted to 14,000 hours because of an unexpected trouble with a microwave neutralizer,[2] in spite of the successfully completed endurance ground-test through 20,000 hours. In order to clarify the causes of performance degradation, the prototype model neutralizer used in the endurance test was reviewed, and it was concluded that the performance degradation was attributed to metal flakes and contamination of the dielectric.[3] Also, the other ground tests for three different geometries of neutralizers showed that the performance and the erosion rate of each wall strongly depend on the geometry.[4] It is considered that the contamination and the erosion were attributed to sputtering by ions, thus the necessity to grasp the ion's behavior is getting increased for the improvement of robustness of the microwave ion engine. Recently, net current into each composing element were measured in order to understand ion's behavior.[5] It was found that a side wall is gathering most of currents than other parts, and an antenna is gathering many electrons.

For further understandings on the discharge phenomena, a numerical solver to simulate the motion of ions in the neutralizer is being developed in this study. In order to simulate the neutralizer with the ion's time/space scales, a Hybrid-PIC(Particle-In-Cell) model was employed, where ions and electrons are models as particles and fluid, respectively. In this paper, the details of the numerical model are described, and the plasma properties such as density and electric potential are discussed. In order to deal with one of the most characteristic phenomena of a microwave neutralizer, we focus on a transition of discharge mode. It is widely known that a microwave neutralizer has two operation modes referred to as low current mode and high current mode, i.e. when a bias voltage exceeds a certain threshold, a discharge current rises discontinuously.[6] In spite of the importance of the mode change, however, little is known about the transition mechanism. To understand the mode transition, two working conditions below and above the threshold voltage are examined under some assumptions, and its characteristics and validity are discussed.

II. Numerical Model

A. Geometry and Computational Region

Figure 1 illustrates a schematic view of a neutralizer simulated in this study, which was assembled at Kyushu University. Although this geometry is not exactly the same as the neutralizer of μ10, qualitative behavior of the microwave plasma will remain unaltered. It has a symmetric discharge chamber with a diameter of 18 mm. A

microwave is fed through a coaxial line followed by an L shaped antenna inserted to the discharge chamber. Because of the asymmetric shape of the antenna, a three dimensional simulation is required to understand realistic physics. Electrons produced by microwave discharge are supposed to be extracted though the orifice with a diameter of 5 mm and an axial length of 8 mm. The configuration was approximated by the Cartesian grids for simplicity as depicted in Fig.2, where the blue colored cells represent a computational region. A grid interval was uniformly set to 0.5 mm which is much shorter than the mean free path of ions. With this grid, although the boundary surface cannot be captured exactly, this resolution will be enough to meet the present purpose to understand overall characteristics of the discharge field. The cavity in the back yoke through which the antenna is inserted was filled by cells belonging to the back yoke for further simplicity.

The computational region was extended by 4 mm toward the plume region, and a virtual anode was located at the boundary surface of x = 28 mm. In actual experiment of this neutralizer, an anode plate was located at 20 mm from the orifice exit, thus direct comparison between the computational and experimental results is impossible. According to a diagnosis, however, there is little potential drop in a plume region, although there may exist an electron sheath about 5-10 V on an anode plate.[7] The outer region between the orifice exit and the virtual anode was removed from the computational region to reduce the calculation cost.

Magnetic field shown in Fig. 3 is applied by a surrounding ring-shaped magnet in order to generate electron's cyclotron motion, which is intended to enhance plasma production. The electrons are trapped by the magnetic field and ionize background neutrals.

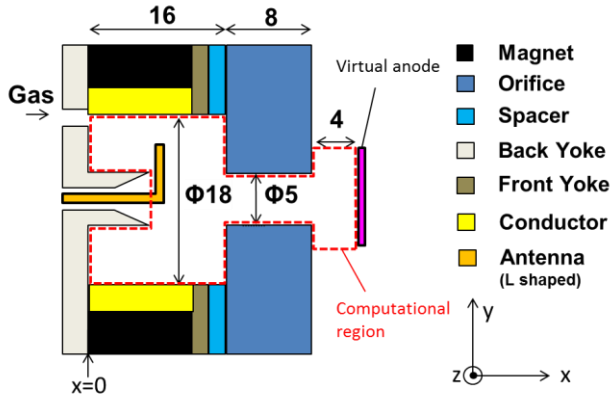

Figure 1. Schematics of Microwave Neutralizer.

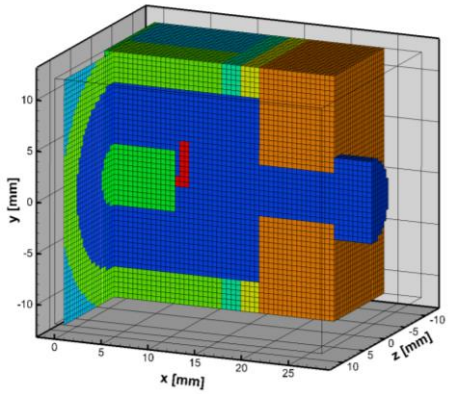

Figure 2. Computational Grid.

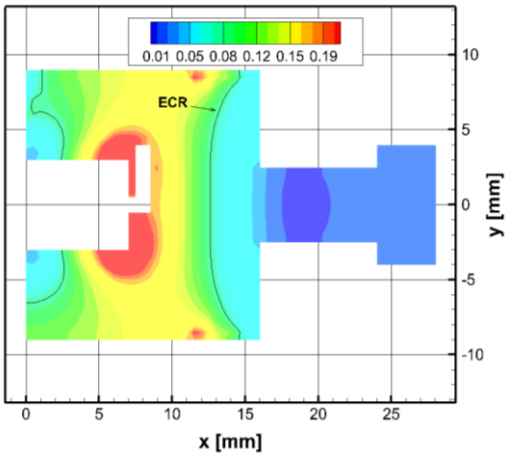

Figure 3. Magnetic field.

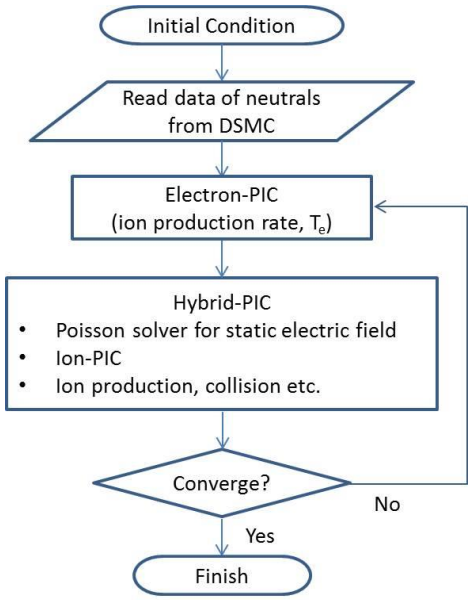

Figure 4. Flow Chart of Calculation.

B. Outline of Numerical Model

In this neutralizer, most of the electrons produced by ionization collisions between electrons and neutrals are ejected from an orifice and reaches the virtual anode. On the other hand, most of the ions are recombined on conductor surfaces with electrons fed from an ion source, and return back to bulk plasma as neutrals; hence the ions plays an important role as a charge carrier in the microwave neutralizer. This indicates that the physics should be modeled in ion's time/space scale to simulate the essential physics of the microwave neutralizer.

Physical properties necessary to model are classified into three categories. First is the ion's motion itself, and second is the static electric field between the neutralizer and the virtual anode. Third is the interaction between the microwave and the electrons, i.e. the process of electron's heating by microwave. The electric power fed through the microwave antenna is absorbed mainly by the electrons, and the energized electrons transfer the power to neutrals by collisions. In particular, when an electron passes through ECR(Electron Cyclotron Resonance) region, the power absorption becomes significant. To simulate such a resonance phenomenon, property of an electron as a particle should be included in the numerical model, because kinetic effects play an important role in the resonance region.

In this study, the first and the second is modeled by Hybrid-PIC(Particle-In-Cell) model which treats ions and electrons as particles and fluid, respectively. The assumption of fluid electron will be obstacle for the modeling of power absorption by ECR. It will be reasonable, however, to understand overall electron's behavior in a discharge chamber, because it was experimentally confirmed that an electron's energy distribution function is Maxwellian under a condition of a low power below 10 W.[6] Regarding the third, interaction between the microwave and the electrons is separately analyzed with an electromagnetic PIC solver developed at Kyushu University.[8] In this solver, only the electrons are traced with PIC method, and the ions as well as the neutrals are treated as background gases. Hereafter, let us refer to this solver as Electron-PIC. This solver provides the production rate of ions and the electron temperature, which are exported to the Hybrid-PIC solver. It has to be noted that the effect of static electric field is ignored in this solver, thus we can extract phenomenological interaction between the microwave and the electrons from the results of the Electron-PIC. In order to consider the ionization related with electron's acceleration by static electric field, Townsend ionization was implemented in a specified region. Since the plasma in the neutralizer is considered to be weakly ionized, the neutrals were treated as background gas whose density was fixed to a result obtained from the preliminary DSMC(Direct Simulation Monte Carlo) analysis. The effect of Coulomb collision between electrons and ions, however, was implemented in the Hyrid-PIC and the Electron-PIC, because it cannot be ignored in comparison with the collisions between electrons and neutrals. The overall flow chart of this simulation is summarized in Fig. 4.

C. Hybrid-PIC Model

In this model, the motion of ions is traced with PIC method.

$$\frac{d\boldsymbol{x}_i}{dt} = \boldsymbol{v}_i, \quad \frac{d\boldsymbol{v}_i}{dt} = \frac{e}{m_i}\left(\boldsymbol{E} + \boldsymbol{v}_i \times \boldsymbol{B}\right) \tag{1}$$

The charge exchange collision and elastic collision with neutrals are taken into account in the ion PIC. The plasma was assumed to be weakly ionized, thus an ion was vanished once it reached a wall to simulate ion's recombination with an electron on a wall. The production rate of ions caused by the microwave discharge is imported from the Electron-PIC code described in the next section. In addition, since the Electron-PIC does not take static electric field into account, ionization by electrons which accelerated by static electric field around orifice exit, i.e. Townsend ionization, has to be implemented separately. This ionization was considered in the Hybrid-PIC, and was incorporated inside the orifice and in the plume region. Then, ions were produced in each cell in accordance with a reaction rate defined as follows.

$$k_f n_n n_e \tag{2}$$

The forward reaction coefficient k_f is a function of electron's mean energy, and was obtained by Bolsig+.[9] In this simulation, the electron's mean energy was defined as a sum of a thermal energy and a mean kinetic energy.

The motion of electrons is expressed by the following drift-diffusion model,

$$\boldsymbol{u}_{e//} = -\mu_e \boldsymbol{E}_{//} - \frac{\mu_e}{e}\frac{\nabla_{//} p_e}{n_e}, \quad \boldsymbol{u}_{e\perp} = \boldsymbol{U}_{e\perp} - \beta_e \boldsymbol{U}_{e\perp} \times \boldsymbol{b} \tag{3}$$

where

$$\boldsymbol{E} = -\nabla\varphi, \quad \mu_\mathrm{e} = \frac{e}{m_e \nu_{eh}}, \quad \boldsymbol{U}_{e\perp} = -\mu_{e\perp}\boldsymbol{E}_\perp - \frac{\mu_{e\perp}}{e}\frac{\nabla_\perp p_e}{n_e}, \quad \mu_{\mathrm{e}\perp} = \frac{\mu_e}{1+\beta_e^2} + \frac{K_B}{16B}, \quad \beta_\mathrm{e} = \frac{eB}{m_e \nu_{eh}}, \quad \boldsymbol{b} = \frac{\boldsymbol{B}}{B}.$$

The mobility perpendicular to the magnetic field includes the effect of Bohm diffusion, where the constant of K_B is fixed to 0.15.[10] The electron's collision frequency includes the collision with ions as well as with neutrals. With this model and the current conservation law,

$$\nabla \cdot \boldsymbol{j} = \nabla \cdot e n_e \left(\boldsymbol{u}_i - \boldsymbol{u}_e \right) = 0 \tag{4}$$

a Poisson equation to yield static electric field can be derived.

$$\nabla \cdot n_e \left\{ \left(\mu_e - \mu_{e,\perp} \right) \left(\boldsymbol{b} \cdot \nabla \varphi \right) \boldsymbol{b} + \mu_{e,\perp} \nabla \varphi - \beta_e \mu_{e,\perp} \nabla \varphi \times \boldsymbol{b} \right\}$$
$$= \nabla \cdot \left\{ n_e \boldsymbol{u}_i + \left(\frac{\mu_e}{e} - \frac{\mu_{e,\perp}}{e} \right) \left(\boldsymbol{b} \cdot \nabla p_e \right) \boldsymbol{b} + \frac{\mu_{e,\perp}}{e} \nabla p_e - \frac{\beta_e \mu_{e,\perp}}{e} \nabla p_e \times \boldsymbol{b} \right\} \tag{5}$$

These formulations are based on the assumption that the static electric field and the microwave electric field can be described separately, i.e. the electric field discussed here represents only a time-averaged static electric field, because the harmonic microwave electric field can be vanished by time-averaging. Such treatment of the electric field is seen in the literature about the microwave discharge simulation.[11-13] Assuming quasi-neutrality, the electron number density is equal to the ion number density obtained from the ion PIC.

The position and the velocity of ions were time-marched with leap-frog method. Equation 5 was discretized with a finite element method, and was solved with a direct method, because the diagonal dominance of obtained linear system is not assured due to high Hall parameter.

It was assumed that all walls are grounded, i.e. the electric potential of the all walls is zero. However, since the Hybrid-PIC model assumes quasi-neutrality, the boundary condition for the electric potential on the walls has to be paid attention. In the vicinity of the walls contacting with plasma, there is a sheath region, where a steep potential drop exists and the assumption of quasi-neutrality becomes invalid. To take the sheath into consideration, a sheath model should be applied to the boundary condition of the electric potential. In this study, the following equality is used as a sheath model,

$$n_e \boldsymbol{u}_e \cdot \boldsymbol{n} = \frac{1}{4} n_e C_e \exp\left(-\frac{e\varphi_{sh}}{kT_e} \right) \tag{6}$$

where $\boldsymbol{n}$ and φ_{sh} denote a normal vector toward a wall surface and a sheath potential, respectively. On the other hand, a potential value of the virtual anode was specified explicitly.

D. Electron-PIC Model

The governing equations of the Electron-PIC are the equation of motion of electrons and Maxwell equation.[8]

$$\frac{d\boldsymbol{x}_e}{dt} = \boldsymbol{v}_e, \quad \frac{d\boldsymbol{v}_e}{dt} = -\frac{e}{m_e} \left(\boldsymbol{E} + \boldsymbol{v}_e \times \boldsymbol{B} \right) \tag{7}$$

$$\nabla \times \boldsymbol{E} = -\mu_0 \frac{\partial \boldsymbol{H}}{\partial t}, \quad \nabla \times \boldsymbol{H} = \varepsilon_0 \frac{\partial \boldsymbol{E}}{\partial t} + \boldsymbol{j}_e \tag{8}$$

Here μ_0 and ε_0 are the permeability and permittivity of vacuum, respectively. Contrary to the Hybrid-PIC formulation, the electric field in Eq. 7 denotes microwave electric field. In the PIC of electrons, elastic, excitation, and ionization collisions between electrons and neutrals were implemented by means of Null-collision method.[14] By counting the ionization collisions, we can estimate the ion production rate per unit time at each cell. In addition, we implemented Coulomb collision between electrons and background ions, because its collision frequency is comparable to that between electrons and neutrals. The electron temperature was determined by

$$T_e = \frac{N_M}{3R_e \left(N_M - 1 \right)} \left(\frac{S}{N_M} - \boldsymbol{V}^2 \right) \tag{9}$$

where

$$N_M = \sum_{m=1}^{M} N^{(m)}, \quad \boldsymbol{V} = \frac{\sum_{m=1}^{M} \sum_{i=1}^{N^{(m)}} \boldsymbol{v}_i^{(m)}}{N_M}, \quad S = \sum_{m=1}^{M} \sum_{i=1}^{N^{(m)}} \left(\boldsymbol{v}_i^{(m)} \right)^2 .$$

Here, M denotes the number of ensemble sampling, and $N^{(m)}$ is the number of super particles in a cell for a sample of m. Since this solver does not include the effect of static electric field, the sheath region should be treated in a special manner. On the boundaries, if an electron's energy is more than a sheath voltage estimated by the Hybrid-PIC, the electron was vanished on the wall, and if not, the electron was reflected without energy loss.

The power of microwave was controlled by the strength of electric field applied at the root of the antenna in the Electron-PIC, i.e. the strength of the electric field at the root of the antenna was adjusted every period so that a temporary input power injected into the plasma approaches a specified power, which can be formulated as,

$$\frac{\partial P'}{\partial t} = \theta\left(P - P'\right) \quad \rightarrow \quad \frac{\partial E}{\partial t} = \theta \frac{E}{2}\left(\frac{P}{P'} - 1\right) \tag{10}$$

where θ, P, and P' are a proportional constant, a specified input power, and a temporary input power calculated by time-integral of a Poynting flux at the root of the antenna. Here, the temporary input power is assumed to be proportional to the square of electric field at the root of the antenna.

E. Calculation Conditions

The calculation conditions are listed in Table 1. In the preliminary DSMC simulation of neutrals, the mass flow rate of a working gas (Xe) was fixed to 0.5 sccm. On the boundaries, a diffuse reflection condition was imposed, where the wall temperature was assumed to be 373 K.

The microwave frequency assumed in the Electron-PIC was 2.45 GHz, thus ECR regions appear at a magnetic flux density of 0.087 T as shown in Fig. 2. The Electron-PIC was time-integrated for 10 ns in each analysis, where the initial electron temperature was set to 2 eV in all cases. The ion production rate and the electron temperature were time-averaged during the latter 5 ns. These time-averaged data were imported in the Hybrid-PIC only in the region upstream of the orifice entrance. The ionization rate interior of the orifice was calculated by Eq. 2, and ionization in the plume region was not modeled. After convergence of the Hybrid-PIC, the ion(electron) number density was fed back to the Electron-PIC.

In this paper, two potential values of the virtual anode were examined. The experimental results of our neutralizer discussed later showed that a transition to a high current mode appears at a bias voltage of 35 V when decreasing the voltage, and at 37.8 V when increasing the voltage. Therefore the potential values of 20 and 38 V were chosen to simulate both a low current mode and a high current mode. According to the plasma diagnosis with electron extraction,[15] the electron temperature in the orifice and plume region is about 3 eV at a low current mode, even though the electron temperature within the discharge chamber is 2 eV. This will be due to the Joule heating by electrons accelerated toward downstream region. It is inferred that the electron temperature in the orifice and the plume region is increased at a high current mode. Hence, in the region downstream of orifice entrance (x > 16 mm), when the anode potential φ_a is 20 and 38 V, the electron temperature was artificially fixed to 3 and 4 eV, respectively. The weight of a super-particle was set to 2.4×10^6 in the Electron-PIC, and in the Hybrid-PIC, 1.25×10^6 and 2.5×10^6 when φ_a = 20 V and 38 V, respectively.

Table 1. Calculation Conditions.

	Case1	Case2
Working gas	Xe	
Mass flow rate	0.5 sccm	
Microwave frequency	2.45 GHz	
Input power	8 W	
Initial electron temperature of Electron-PIC	2 eV	
Potential of virtual anode	20 V	38 V
Electron temperature in x > 16mm	3 eV	4 eV

III. Results and Discussion

A. Neutral Density

Figure 5 shows the number density and axial velocity distributions of the neutrals obtained by the DSMC analysis. Around the antenna, the density is about 4×10^{20} m^{-3}. This value is consistent with rough estimation of a number density by use of the mass flow rate and a conductance modified with Clausing's factor. Since the present aspect ratio of the orifice is L/D=1.6, the Clausing's factor is estimated about 0.4. Then, assuming T = 373 K in the neutralizer and p = 0 Pa in the plume region, the estimated number density in the neutralizer is 3.4 $\times10^{20}$ m^{-3}, thus the simulated result seems reasonable. The mean free path of neutrals is about 12 mm, which leads to a Knudsen number about unity. The number density diminishes gradually though the orifice, and rapidly decreases down to 10^{18}-10^{19} m^{-3} in the plume region.

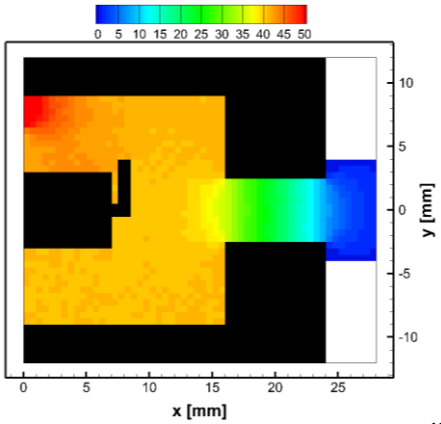

Figure 5. Number density of neutrals, 10^{19} m^{-3}.

B. Plasma Properties

The ion density distributions at the symmetric plume (z = 0 mm) are shown in Fig. 6. In both cases, high ion density region is formed between the tip of the antenna and the front yoke. According to a photograph taken from downstream side in Ref.6, the intensity of emission is highest around the antenna, which will assure the validity of the simulation result. A cut off density of 2.45 GHz microwave is 7.45×10^{16} m^{-3}, thus the plasma around the antenna is in the state of over-dense condition, which was also confirmed experimentally by means of a probe measurement.[4,6] The oblique distribution of the high density region is due to the high ionization rate in this region. Figure 7 shows the ionization sites during 5 ns obtained by Electron-PIC. In this figure, ionization sites between -2 < z < 2 mm are plotted. It can be seen that many ionization collisions occur between the tip of the antenna and the front yoke. It is considered that highly energized electrons are trapped to the magnetic field, and directly ionize neutrals during bouncing motions, which is suggested by the electron temperature distribution shown in Fig. 8 obtained by Electron-PIC. The electron temperature amounts to 5 eV around the antenna, and a band of high temperature region of 3-4 eV is formed between the antenna and the front yoke. In the Case2, the density has a peak between the antenna and the back yoke. It is considered that produced electrons tend to be accumulated in this region, since the tip of the antenna is relatively close to the high magnetic field region around the back yoke.

In spite of the same calculation condition of Electron-PIC in both cases, the amount of ion productions by microwave discharge is considerably increased in Case2. This will be attributed to additional ions supplied from the orifice region. In the orifice and the plume region, the Townsend ionization makes the ion density increased up to 1 $\times10^{18}$ m^{-3} in both Cases. Even though the amount of ion production inside the orifice was less than the half of ion production by microwave discharge, the Townsend ionization has a significant impact on the microwave discharge. The result implies that the increase in the ion production rate at the high current mode is not strongly related with the electron's energy but with the grown density, because the electron temperature around the antenna is nearly the same in both cases.

Figure 9 shows the electric potential distributions. It can be seen that the high potential region appears between the antenna and the front yoke like the density distribution. The similarity between the density and the potential distribution suggests that the density is approximately linked with the electric potential by Boltzmann relation along the magnetic field. The ions produced between the antenna and the front yoke is radially accelerated by this potential gradient. In the region downstream of the orifice entrance, however, the potential gradually increases toward the virtual anode. Therefore ions produced by the microwave discharge hardly reach the orifice exit. Most of the ions ejected toward the plume region originate from Townsend ionization around the orifice exit.

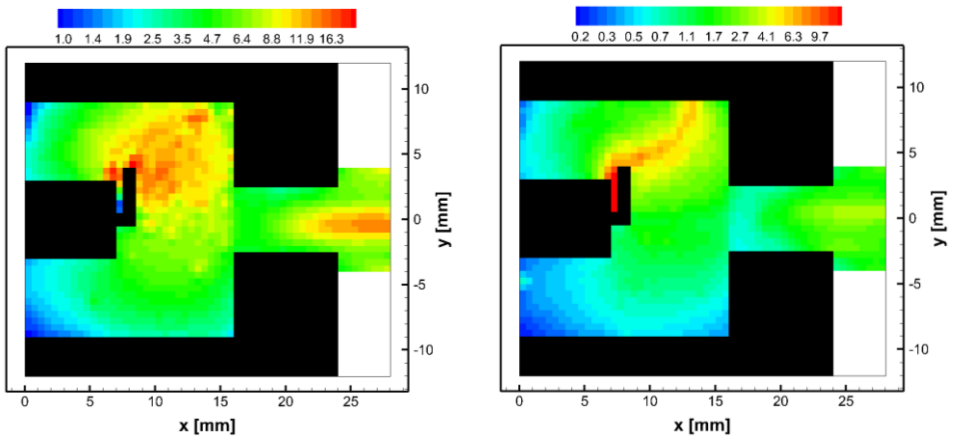

(a)Case1: Low current mode (φ_a = 20 V) (b)Case2: High current mode (φ_a = 38 V)

Figure 6. Number density of ions, (a): in 10^{17} m^{-3}, (b): in 10^{18} m^{-3}.

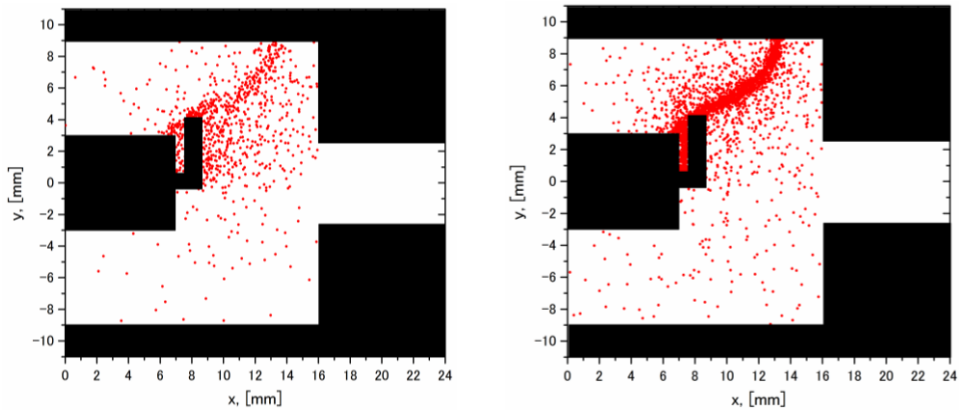

(a)Case1: Low current mode (φ_a = 20 V) (b)Case2: High current mode (φ_a = 38 V)

Figure 7. Ionization collision sites obtained by Electron-PIC during 5 ns: *Ionization sites between -2 mm < z < 2 mm are plotted. Ionization sites inside the orifice are ignored in these figures.*

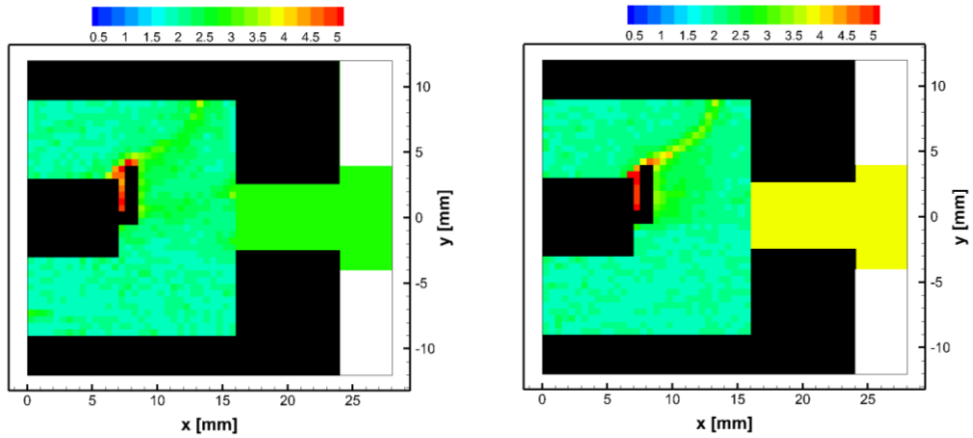

(a)Case1: Low current mode (φ_a = 20 V) (b) Case2: High current mode (φ_a = 38 V)

Figure 8. Electron temperature, eV : *In x < 16 mm, the electron temperature obtained by Electron-PIC is shown. In x > 16 mm, the electron temperature was artificially fixed to 3 eV and 4 eV in Case1 and Case2, respectively.*

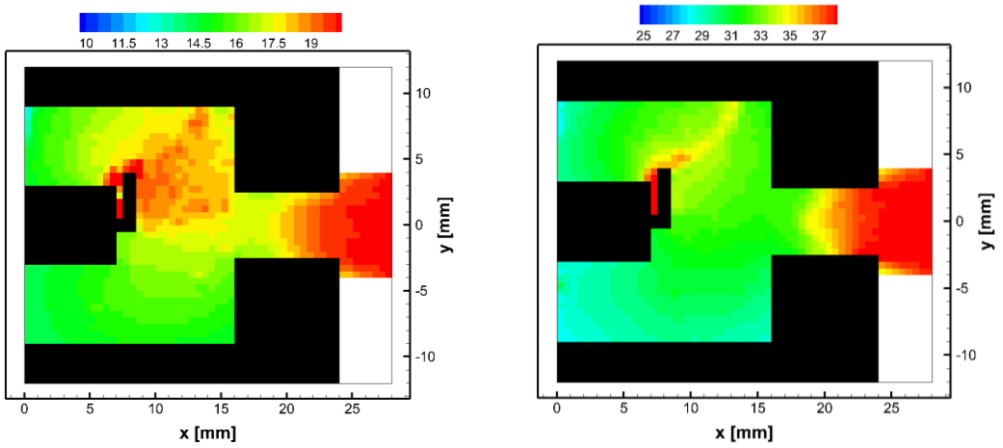

(a)Case1: Low current mode (φ_a = 20 V) (b)Case2: High current mode (φ_a = 38 V)

Figure 9. Electric Potential, V.

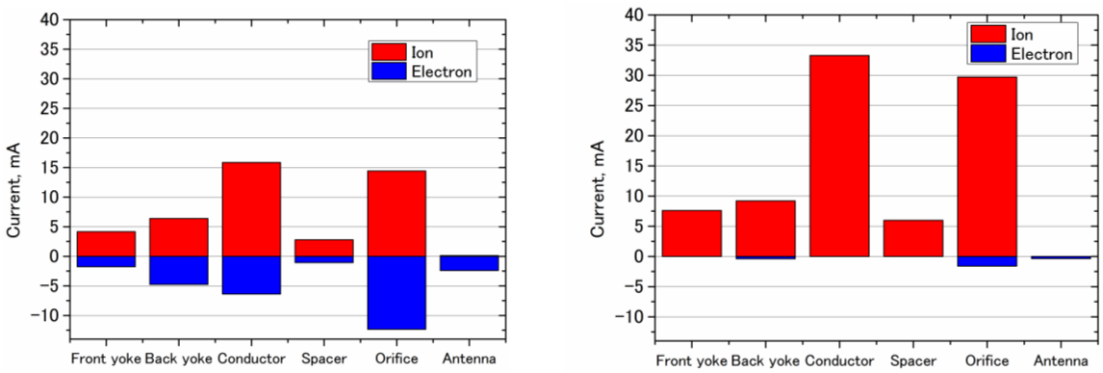

(a)Case1: Low current mode (φ_a = 20 V) (b)Case2: High current mode (φ_a = 38 V)

Figure 10. Current into each component.

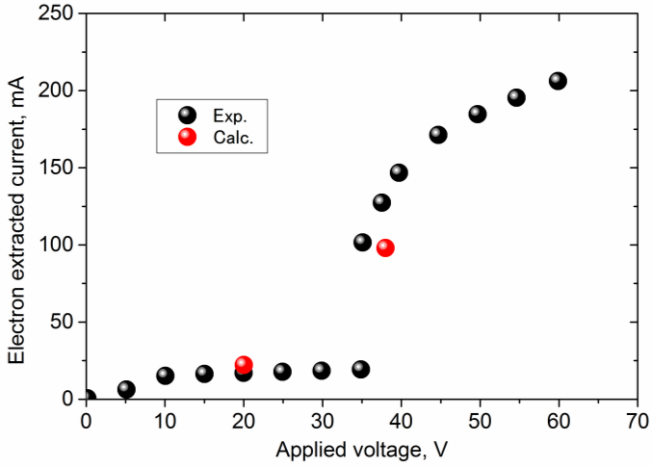

Figure 11. Voltage-Current Characteristics.

C. Current Distribution

The ions produced mainly between the tip of the antenna and the front yoke are accelerated radially by the static electric field, and flow in the chamber wall. From the simulation results, the ion and electron currents into each component were calculated as shown in Fig. 10 (also see Fig. 1). The electron current was estimated by means of Eq.

6. It is remarkable that, in Case1, the electron current is dominant at the antenna due to the high electron temperature around the antenna, i.e. highly energized electrons can overcome the sheath potential on the antenna. This feature was also observed in the experiment of μ10 neutralizer.[5] The amount of the electron current is quite large on the orifice due to its large surface area and assumed high electron temperature. On the other hand, in Case2, electron currents into each component are almost zero due to a large sheath potential on the walls, since the higher bias voltage leads to higher electric potential within the discharge chamber. Comparing the Case1 with the Case2, increasing rate of the ion current into the orifice is the highest in all components. This is attributed to the enhanced ionization inside the orifice.

D. Voltage-Current Characteristics

The neutralization current is compared with the experimental data obtained by authors at Kyushu University. In the experiment, an anode plate was located 20 mm apart from the orifice exit. Figure 11 shows the obtained voltage-current characteristics, and simulated values are also plotted. The simulated values were estimated by integrating electron flux defined by Eq. 6 on the virtual anode. It should be noted that the bias voltage of the simulation does not correspond to the bias voltage of the experiment because of the different plume length and existence of an anode sheath. Even though the potential gradient in the plume region is quite moderate, the sum of the potential drop in the remaining plume region and an anode sheath drop will be 5-10 V.[7] Therefore the current should be compared with the experiment at a higher bias voltage about 5-10 V. The simulation results, however, are plotted at a potential of the virtual anode because of the uncertainty of the potential drop in the remaining plume region and the anode sheath.

The simulation result of Case1 agrees well with the experimental data, even allowing for the uncertain surplus potential drop because the discharge current is almost constant at the low current mode. The agreement with the experimental value suggests that there is little ionization processes in the remaining plume region. On the other hand, in Case2, the simulation underestimates the extraction current in light of the remaining plume region. The experimental value, however, will contain the electrons produced in the remaining plume region. Therefore, the underestimation of the current may be justified. For further understanding, not only a simulation of the discharge chamber but also a plume analysis will be necessary.

IV. Conclusion

The three dimensional Hybrid-PIC solver has been developed to simulate a microwave neutralizer in the ion's time/space scales. The microwave discharge was modeled with another electromagnetic code referred to as Electron-PIC, which can provide the Hybrid-PIC with the local ion production rate and the electron temperature. In the orifice and the plume region, Townsend ionization was taken into account in place of the ionization rate given by the Electron-PIC to simulate ionization with regard to accelerated electrons. In order to deal with one of the most characteristic phenomena of a microwave neutralizer, we focused on a transition of discharge mode; from low current mode to high current mode.

Under the condition of a mass flow rate of 0.5 sccm, a microwave power of 8 W, and a microwave frequency of 2.45 GHz, a bias voltage applied to a virtual anode was set to 20 V and 38 V to simulate the low current mode and the high current mode, respectively. In both cases, there appears a high density region between the antenna and the front yoke due to high ionization rate caused by energized bouncing electrons. In the region downstream of the orifice entrance, the ion density is gradually increased and amounts to over 1×10^{18} m^{-3} due to Townsend ionization, which result in a positive gradient of electric potential toward downstream region.

At the low current mode, the electrons losses are significant on the orifice surface because of its large surface area and the assumed high electron temperature inside the orifice. At the antenna, an electron current is dominant due to the high electron temperature around the antenna. A simulated electron extraction current of 22 mA agrees well with the experimental data even allowing for the potential drop in the remaining plume region ignored in the simulation. At the high current mode, the electron losses become reduced due to a high sheath potential sustained by the high bias voltage. A simulated electron extraction current of 98 mA underestimates the experimental value, which is probably due to the electron production in the remaining plume region.

References

[1]Nishiyama, K., Hosoda, S., Koizumi, H., Shimizu, Y., Funaki, I., Kuninaka, H., Bodendorfer, M., Kawaguchi, J., and Nakata, D., "Hayabusa's Way Back to Earth by Microwave Discharge Ion Engines," AIAA-2010-6862, 2010.

[2]Hosoda, S., and Kuninaka, H., "The Homeward Journey of Asteroid Explorer "Hayabusa" Powered by the Ion Engine," *Journal of Plasma and Fusion Research*, Vol. 86, pp.282-292, 2010. (in Japanese)

[3]Ohmichi, W., and Kuninaka, H., "Degradation Mechanism of ECR Neutralizer and Countermeasure," IEPC-2011-314, 2011.

[4]Satori, S., Funaki, I., and Kuninaka, H., "Plasma Diagnostics of Microwave Neutralizer," *Journal of the Japan Society for Aeronautical and Space Sciences*, Vol. 47, pp. 197-201, 1999. (in Japanese)

[5]Ohmichi, W., and Kuninaka, H., "Ion Current Distribution of ECR Microwave Discharge Neutralizer," AIAA-2012-4192, 2012.

[6]Funaki, I., and Kuninaka, H., "Overdense Plasma Production in a Low-Power Microwave Discharge Electron Source," *Japanese Journal of Applied Physics*, Vol. 40, pp. 2495-2500, 2001.

[7]Kuninaka, H., and Nishiyama, K., "Development of 20cm Diameter Microwave Discharge Ion Engine μ20," AIAA-2003-5011, 2003.

[8]Masui, H., Tashiro, Y., Yamamoto, N., Nakashima, H, and Funaki, I., "Analysis of Electron and Microwave Behavior in Microwave Discharge Neutralizer," *Transactions of the Japan Society for Aeronautical and Space Sciences*, Vol. 49, pp. 87-93, 2006.

[9]Hagelaar, G. J. M., Pitchford, L. C., "Solving the Boltzmann equation to obtain electron transport coefficients and rate coefficients for fluid models," *Plasma Sources Science and Technology*, Vol. 14, pp. 722-733, 2005.

[10]Fife, J. M., "Nonlinear Hybrid-PIC Modeling and Electrostatic Prove Survey of Hall Thrusters," Ph. D. Dissertation, Aeronautics and Astronautics Dept., Massachusetts Institute of Technology, Cambridge, MA, 1998.

[11]Yasaka, Y., Fukuyama, A., Hatta, A., and Itatani, R., "Two-dimensional Modeling of Electron Cyclotron Resonance Plasma Production," *Journal of Applied Physics*, Vol.72, No. 7, pp. 2652-2658, 1992.

[12]Williamson, M. C., Lichtenberg, A. J., and Lieberman, M. A., "Self-consistent Electron Cyclotron Resonance Absorption in a Plamsa with Varying Parameters," *Journal of Applied Physics*, Vol. 72, No. 9, 1992.

[13]Yasaka, Y., and Uda, N., "Practical Scheme for Three-dimensional Simulation of Electron Cyclotron Resonance Plasma Reactors," *Journal of Applied Physics*, Vol. 89, No. 7, pp. 3594-3601, 2001.

[14]Vahedi, V., and Surendra, M., "A Monte Carlo Collision Model for the Particle-In-Cell Method: Applications to Argon and Oxygen Discharges," *Computer Physics Communications*, Vol. 87, No. 179, 1995.

[15]Onodera, N., Takegahara, H., Nishiyama, K., Funaki, I., and Kuninaka, H., "Electron Emission Mechanism of Microwave Discharge Neutralizer," *Journal of the Japan Society for Aeronautical and Space Sciences*, Vol. 49, pp. 27-31, 2002. (in Japanese)